

## Full Articles

### Optimization of signal-to-noise ratio in the *in vivo* $^{31}\text{P}$ magnetic resonance spectra of the human brain

A. V. Manzhurtsev,<sup>a,b\*</sup> N. A. Semenova,<sup>a,b,c</sup> T. A. Akhadov,<sup>b</sup> O. V. Bozhko,<sup>b</sup> and S. D. Varfolomeev<sup>a</sup>

<sup>a</sup>Emanuel Institute of Biochemical Physics, Russian Academy of Sciences,  
4 ul. Kosygina, 119334 Moscow, Russian Federation  
E-mail: andrey.man.93@gmail.com

<sup>b</sup>Research Institute of Children Emergency Surgery and Trauma,  
22 ul. Bolshaya Polyanka, 119180 Moscow, Russian Federation

<sup>c</sup>N. N. Semenov Institute of Chemical Physics, Russian Academy of Sciences,  
4 ul. Kosygina, 119334 Moscow, Russian Federation

The main problem in  $^{31}\text{P}$  magnetic resonance spectroscopy is a low signal-to-noise ratio (SNR) of spectra acquired with clinical magnetic resonance imaging (MRI) scanners. Using spin-spin phosphorus-proton ( $^{31}\text{P}$ – $^1\text{H}$ ) decoupling and heteronuclear Overhauser effect and taking into account the effect of the longitudinal relaxation time  $T_1$  on the SNR, the method for localization and excitation of the region of interest (Image Selected *in vivo* Spectroscopy pulse sequence) was optimized to increase the SNR in the  $^{31}\text{P}$  magnetic resonance spectra of the human brain to ~50% without increasing signal acquisition time.

**Key words:**  $^{31}\text{P}$  magnetic resonance spectroscopy, signal-to-noise ratio (SNR), proton decoupling, nuclear Overhauser effect, repetition time (TR).

$^{31}\text{P}$  magnetic resonance spectroscopy (MRS) is a unique method for *in vivo* studies of energy and lipid exchange in human organs and tissues. The method is highly efficient in studies of exchange processes in health and in disease including analysis of brain energy metabolism disturbance under ischemic injury and reperfusion,<sup>1</sup> deviations of phospholipid profiles in tumors,<sup>2</sup> and the response of energy metabolism to neurostimulation in local brain zones.<sup>3,4</sup>

Magnetic resonance spectroscopy on  $^{31}\text{P}$  nuclei offers a number of advantages over  $^1\text{H}$  MRS that is traditionally used for *in vivo* studies of human metabolism. These in-

clude a wide range of chemical shifts and no need to suppress the signal of water. However, the application of  $^{31}\text{P}$  MRS is essentially complicated by a low sensitivity of the method. The magnetic susceptibility of phosphorus nuclei is by a factor of 2.5 lower than that of protons, thus being a key problem in *in vivo*  $^{31}\text{P}$  MRS, *viz.*, the need to increase the region of interest and the spectral acquisition time in order to achieve reasonably high values of the signal-to-noise ratio (SNR).

The highest SNR values in the  $^{31}\text{P}$  magnetic resonance spectra of the human brain are obtained for signals of the

phosphate groups of the participants of energy metabolism, namely, phosphocreatine (PCr, chemical shift  $\delta$  0) and ATP ( $\beta$ -ATP,  $\delta \sim -16.7$ ;  $\alpha$ -ATP,  $\delta \sim -7.6$ ;  $\gamma$ -ATP,  $\delta \sim -2.6$ ). The resonance line of  $\gamma$ -ATP overlaps that of  $\beta$ -adenosine diphosphate ( $\beta$ -ADP) while the peak of  $\alpha$ -ATP overlaps the lines of  $\alpha$ -ADP, nicotinamide adenine dinucleotide (NAD(H)), and uridine diphosphate glucose (UDPG). The spectrum also exhibits signals for inorganic phosphate ( $P_i$ ,  $\delta \sim 4.7$ ) and participants of lipid exchange, *viz.*, phosphomonoesters (PME,  $\delta \sim 6.4$ ) and phosphodiester (PDE,  $\delta \sim 3.5$ ). Low intensity of the  $P_i$  signal deteriorates the quality of *in vivo* pH measurements since the most accurate method for the determination of the local intracellular pH values from  $^{31}\text{P}$  magnetic resonance data is to evaluate the shift,  $\delta$ , of the  $P_i$  signal relative to the PCr signal.<sup>5</sup> This also complicates a separate analysis of the intensities of the signals of phosphoethanolamine (PE,  $\delta \sim 6.7$ ) and phosphocholine (PC,  $\delta \sim 6.2$ ) contributing to the PME peak, as well as quantitative processing of the signals of glycerophosphoethanolamine (GPE,  $\delta \sim 3.7$ ), glycerophosphocholine (GPC,  $\delta \sim 3.0$ ) and unidentified phosphodiester (GPX,  $\delta \sim 2.8$ ) contributing to the PDE peak.

The sensitivity improvement methods for  $^{31}\text{P}$  nuclei are based on irradiation of the system under study with radiofrequency (RF) pulses at the resonance frequencies of both phosphorus nuclei and protons. These are proton decoupling<sup>6</sup> and the nuclear Overhauser effect (nuclear Overhauser enhancement, NOE).<sup>7</sup> The former makes use of spin-spin coupling between phosphorus nuclei and protons which causes the excited energy levels of  $^{31}\text{P}$  nucleus to split. Correspondingly, the  $^{31}\text{P}$  resonance signal becomes split into a multiplet with weaker components. Irradiation at the proton frequency when detecting the  $^{31}\text{P}$  signal suppresses the  $^{31}\text{P}$ – $^1\text{H}$  spin-spin coupling and, therefore, the splitting, thus enhancing the signal detected. In the case of the NOE, one deals with direct dipole-dipole coupling between  $^{31}\text{P}$  nuclei and protons. This makes it possible to increase the population difference between the low- and high-energy levels of  $^{31}\text{P}$  nuclei and thus to increase the number of  $^{31}\text{P}$  nuclei involved in the formation of the resonance signal owing to irradiation at the proton resonance frequency.

Both methods have been well studied theoretically and are widely used in nuclear magnetic resonance (NMR) spectroscopy. However, unlike NMR spectroscopy, application of these approaches in localized *in vivo*  $^{31}\text{P}$  magnetic resonance spectra requires optimization from the standpoint of time cost, first of all, because the subjects are humans. Such recording parameters, as the repetition time (TR) and the number of signal averaging (NSA) provide a SNR gain through longer duration of the study. By increasing the SNR using other procedures one can decrease the TR and NSA values and, therefore, make the overall procedure less time-consuming.

The aim of this work is to obtain high-SNR  $^{31}\text{P}$  magnetic resonance spectra at minimum data acquisition time. Thus the study is to a great extent methodological, that is, it presents the scenarios for choosing parameters of  $^{31}\text{P}$  MR spectra that are optimal for clinical practice.

## Experimental

**Volunteers.** Eleven (six male and five female) healthy subjects (age range 18–50 years) were enrolled in the study. All of them passed a standard diagnostic magnetic resonance imaging (MRI) examination on a Philips Achieva 3.0 T system, including  $T_2$ -,  $T_1$ -, diffusion-weighted, and fluid attenuation inversion–recovery (FLAIR) images. The absence of structural abnormalities according to the MRI data served as the study entry criterion.

**$^{31}\text{P}$  magnetic resonance study.** Spectroscopic study was carried out using a transmit–receive head RF  $^{31}\text{P}/^1\text{H}$  bird cage coil (Rapid Biomedical, Germany). The  $^{31}\text{P}$  MR spectroscopy voxel was positioned using the 3D survey images and a set of 2D axial images.

Taking account of the chemical shift displacement artifact (CSDA) for all metabolites,<sup>8</sup> the spectroscopic volume of interest (voxel) of size 80S60S60 mm was located in such a manner that it will be maximally immersed into the brain tissue. To take account of the CSDA, voxel positioning is performed using the parameters "Reference metabolite" and "shifted metabolite displayed". In this case, two frames are shown, one corresponding to the voxel of the reference metabolite and the other corresponding to the voxel of the metabolite with a known  $\delta$  value. Therefore, signals appeared between the resonance lines chosen will be detected from the voxels located between the two frames. Positioning was performed in such a manner that the frames for PE and  $\beta$ -ATP (these metabolites correspond to the outermost lines in the  $^{31}\text{P}$  spectrum of the human brain) be within the brain tissue. An example is shown in Fig. 1.

The STEAM and PRESS pulse sequences (PS) traditionally used in  $^1\text{H}$  MRS are not employed in  $^{31}\text{P}$  MRS since in the latter case the echo signal is detected the time TE after application of the excitation radiofrequency (RF) pulse. Owing to short relaxation times  $T_2$  of  $^{31}\text{P}$  signals the echo signal appears to be much weaker than the free induction decay (FID) signal.<sup>9</sup> Therefore, voxel localization was performed using the Image Selected *in vivo* Spectroscopy (ISIS) PS with the following parameters: echo time (TE) 0.1 ms, number of spectral points 1024, spectral bandwidth (BW) 4000 Hz; the number of dummy scans necessary to attain the equilibrium magnetization was 2. This PS is more efficient in the case of heteronuclear MRS.<sup>10</sup>

The flip angle (FA) of the total magnetization vector was chosen to be 35°. Theoretically, obtaining the maximum SNR requires that FA be set equal to the Ernst angle for each metabolite. However, a large scatter of the  $T_1$  relaxation times<sup>11</sup> precludes the choice of a certain FA value for all metabolites while acquisition of a set of spectra at different FA values elongates the study time, which is unacceptable in clinical practice. Our tests carried out using increased FA values equal to 45°, 60°, and 90° were accompanied by a gradual decrease in the  $\beta$ -ATP signal intensity up to complete disappearance, probably, due to narrowing of the bandwidth irradiated. That is why we decided to use a flip angle of 35°, at which the  $\beta$ -ATP signal intensity is high enough for reliable quantitative data processing and for variation of other parameters.

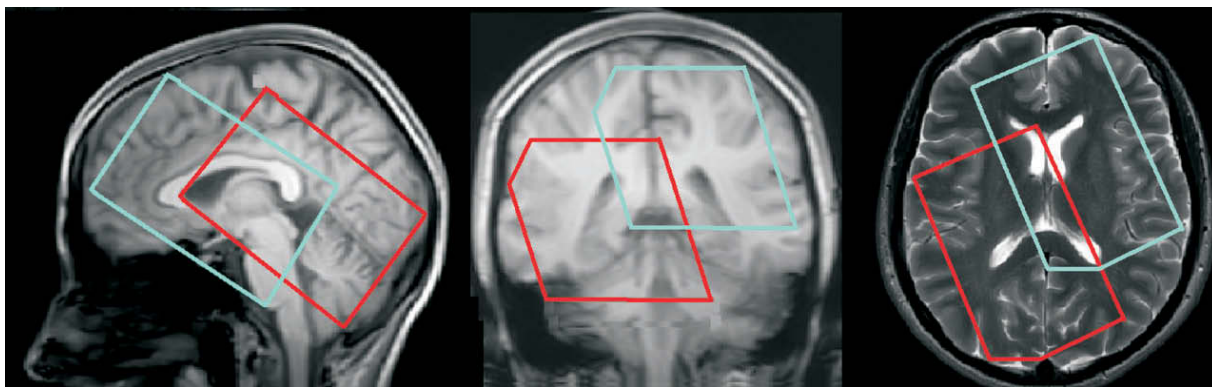


**Fig. 1.** Spectroscopic voxel location in brain tissue. The red frame (closer to the back of the head) characterizes the volume from which the signal of the reference metabolite (PE) is detected, while the blue frame (closer to the forehead) displays the source of the  $\beta$ -ATP signal chemically displaced from the signal of the reference metabolite. For details, see text.

*Note.* Figures 1 and 2 are available in full color on the web page of the journal (<http://www.link.springer.com>).

To increase the SNR, the ISIS PS was modified as follows:

- by including broadband proton decoupling using the Waltz 4 PS;<sup>12</sup> the maximum RF field strength ( $B_{1\text{max}}$ ) was 2.3  $\mu\text{T}$  and the decoupling time was 237 ms;

- broadband proton irradiation over certain period of time before application of the  $^{31}\text{P}$  excitation pulse to implement the NOE using the Waltz 16 PS (see Ref. 13) at  $B_{1\text{max}} = 2.84 \mu\text{T}$ .

Compared to simple repetitive irradiation at the proton resonance frequency, these pulse sequences are more efficient at lower RF energy transmitted.<sup>12</sup> The modified ISIS PS used in this work is shown in Fig. 2.

Our study on the SNR gain in the  $^{31}\text{P}$  spectra involved three sets of measurements. In the first set, four spectra were recorded, (i) without proton decoupling and NOE, (ii) with proton decoupling only, (iii) with NOE only, and (iv) with both proton decoupling and NOE. For all spectra, the relaxation time delay, TR, was 2000 ms, the mixing time in the measurements with NOE was 1600 ms, and NSA was 128. The duration of the first set was 17 min 4 s.

In the second set of measurements, a conventional ISIS PS without proton decoupling and NOE was applied to acquire three spectra with the parameters NSA = 64 and TR = 2, 3, and 4 s.

Depending on the TR value, the spectrum acquisition time varied from 2 min 12 s to 4 min 24 s. The duration of the second set was 9 min 54 s.

The third set of measurements with proton decoupling and NOE was carried out using fixed values of the parameters TR = 3 s and NSA = 64 (see Fig. 2). Spectral data were acquired at mixing times equal to 0, 250, 500, 750, 1000, 1250, 1500, 1750, 2000, 2250, and 2500 ms. The duration of the third set was 36 min 18 s.

The RF field homogeneity in the region of interest was automatically adjusted before each set of measurements using first- and second-order shim coils. Thus, all data sets to be processed and compared were acquired at the same field homogeneity accurate to thermal fluctuations and small-amplitude involuntary movements of the volunteers, which was non-essential at such a large size of the spectroscopic voxel.

The large voxel size was specially chosen to make all resonance lines in the spectra acquired using non-optimum parameters accessible to quantitative processing, like the lines in the spectra obtained using optimum parameters, because an exact comparison of the SNR is possible only in this case.

To optimize the conventional and modified ISIS PS, the NSA value used in all sets of measurements was a multiple of 32 since

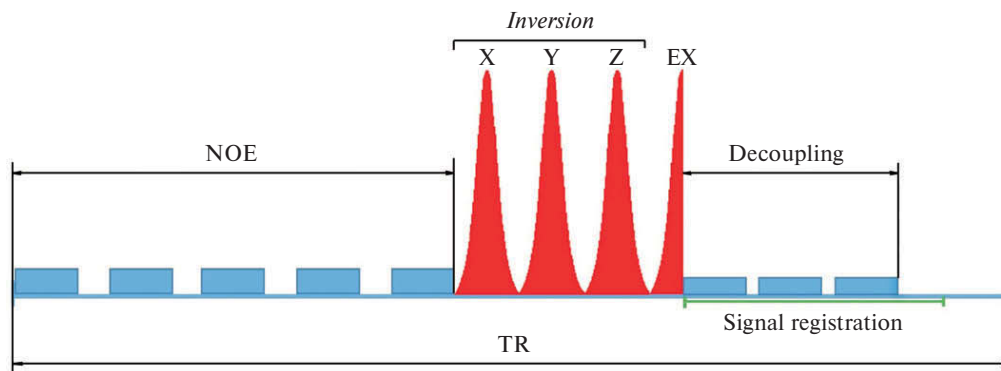


**Fig. 2.** A schematic of modified ISIS pulse sequence; Inversion denotes application of inversion pulses in the presence of gradients along the X, Y, and Z; EX is the excitation pulse, and Signal registration is the signal acquisition time. Blue rectangles on the left and on the right of the red "pulses" Inversion and EX denote irradiation at the proton resonance frequency.

this parameter should be a multiple of the number of phase cycles in the ISIS and Waltz 4 pulse sequences, *i.e.*, 8S4.

**Data processing.** Spectra were processed using the Spectroview program incorporated into the Philips Achieva 3.0 T software.

For each set of measurements, we determined the SNR values for each resonance line in the spectrum. In the first set, the SNR values of the resonances from the proton decoupled spectra ( $\text{SNR}_{\text{dec}}$ ), from the spectra with the NOE ( $\text{SNR}_{\text{NOE}}$ ), and from the spectra recorded using both proton decoupling and NOE ( $\text{SNR}_{\text{total}}$ ) were normalized to the corresponding values for the spectra acquired without proton decoupling and NOE ( $\text{SNR}_{\text{init}}$ ).

In the second set of measurements, for each volunteer and all signals we calculated the SNR gain (in %) upon an increase in TR from 2 to 3 and 4 s, as well as from 3 to 4 s.

In the third set of measurements, the SNR values for each peak obtained at different mixing times were normalized to corresponding values acquired at a mixing time of zero.

A statistical analysis was carried out using the Mann–Whitney U-test incorporated into the STATISTICA 12 program at a significance level of  $p < 0.05$ .

## Results and Discussion

Typical spectra recorded at TR = 3000 ms and NSA = 64 with and without proton decoupling and NOE are presented in Fig. 3. The same Gaussian and exponential apodization was applied to the spectra, so noise smoothing was performed identically and differences between the residual noise in the spectra are accounted for by the signal intensities. Even a visual comparison suggests that application of the NOE and proton decoupling improves the SNR.

**Results of the first set of measurements.** The results obtained in the first set of measurements (see Tables 1 and 2)

**Table 1.**  $\text{SNR}_{\text{dec}}/\text{SNR}_{\text{init}}$  and  $\text{SNR}_{\text{NOE}}/\text{SNR}_{\text{init}}$  ratios for signals in the  $^{31}\text{P}$  magnetic resonance spectrum of the human brain\*

Signal	$\text{SNR}_{\text{dec}}/\text{SNR}_{\text{init}}$	SD	$\text{SNR}_{\text{NOE}}/\text{SNR}_{\text{init}}$	SD
PCr	1.21**	0.16	1.20**	0.15
$\gamma$ -ATP	1.11**	0.11	0.96	0.15
$\alpha$ -ATP	1.17	0.15	1.07	0.15
$\beta$ -ATP	1.12**	0.10	1.01	0.23
$\text{P}_i$	1.25**	0.17	1.05	0.28
PE	1.75**	0.33	1.75**	0.41
PC	1.13	0.52	0.97	0.51
GPE	1.12	0.51	1.37	0.79
GPC	1.16	0.20	1.58	0.54
GPX	1.03	0.30	1.31	0.55
DN	1.59	1.12	1.55**	0.62

\* SD is standard deviation;  $\gamma$ -,  $\alpha$ -,  $\beta$ -ATP denote three resonance lines of ATP; GPE is glycerophosphoethanolamine; and DN stands for dinucleotides.

\*\* Statistically significant gain ( $p < 0.05$  according to Mann–Whitney U-test).

allow one to evaluate the effectiveness of proton decoupling and NOE. The data in Tables 1 and 2 demonstrate the effects of separate and combined application of proton decoupling and NOE. Averaging over all volunteers shows that both parameters improve the SNR for the metabolites studied (average SNR gain was about 24% for proton decoupling and about 26% for NOE), although the effect is not always statistically significant.

Combined application of proton decoupling and NOE led to an average SNR gain of about 51%, which was statistically significant for almost all metabolites.

**Results of the second set of measurements.** The SNR gain (in per cent) for all peaks in the  $^{31}\text{P}$  magnetic reso-

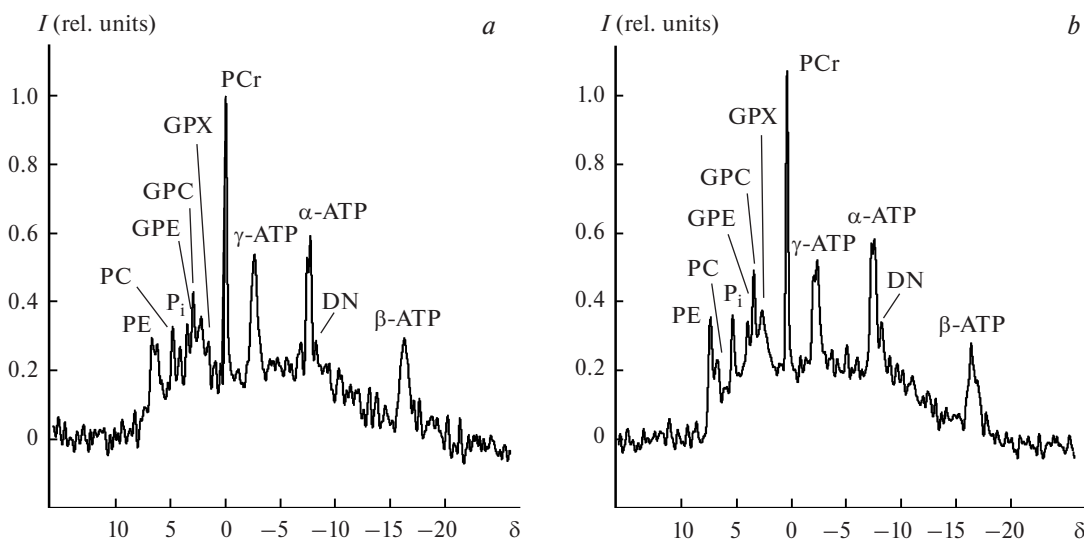


**Fig. 3.** Spectra acquired using conventional (a) and modified (b) ISIS PS. The vertical scale for both spectra is normalized to the signal amplitude of PCr in spectrum a.

**Table 2.**  $\text{SNR}_{\text{total}}/\text{SNR}_{\text{init}}$  ratios for signals in  $^{31}\text{P}$  magnetic resonance spectrum of the human brain

Signal	$\text{SNR}_{\text{total}}/\text{SNR}_{\text{init}}$	SD
PCr	1.54*	0.29
$\gamma$ -ATP	1.16*	0.25
$\alpha$ -ATP	1.26*	0.20
$\beta$ -ATP	1.09	0.12
$\text{P}_i$	1.47*	0.21
PE	1.83*	0.34
PC	1.47*	0.31
GPE	1.67*	1.70
GPC	1.93	1.29
GPX	1.66	1.42
DN	1.58*	0.33

\* Statistically significant ( $p < 0.05$  according to Mann–Whitney U-test).

nance spectrum obtained at all TR values can be seen in Table 3. Clearly, the longer the time TR the larger the SNR. However, for some metabolites and pairs of the TR values being compared the SNR gain thus obtained does not exceed that obtained by increasing the NSA value at shorter times TR.

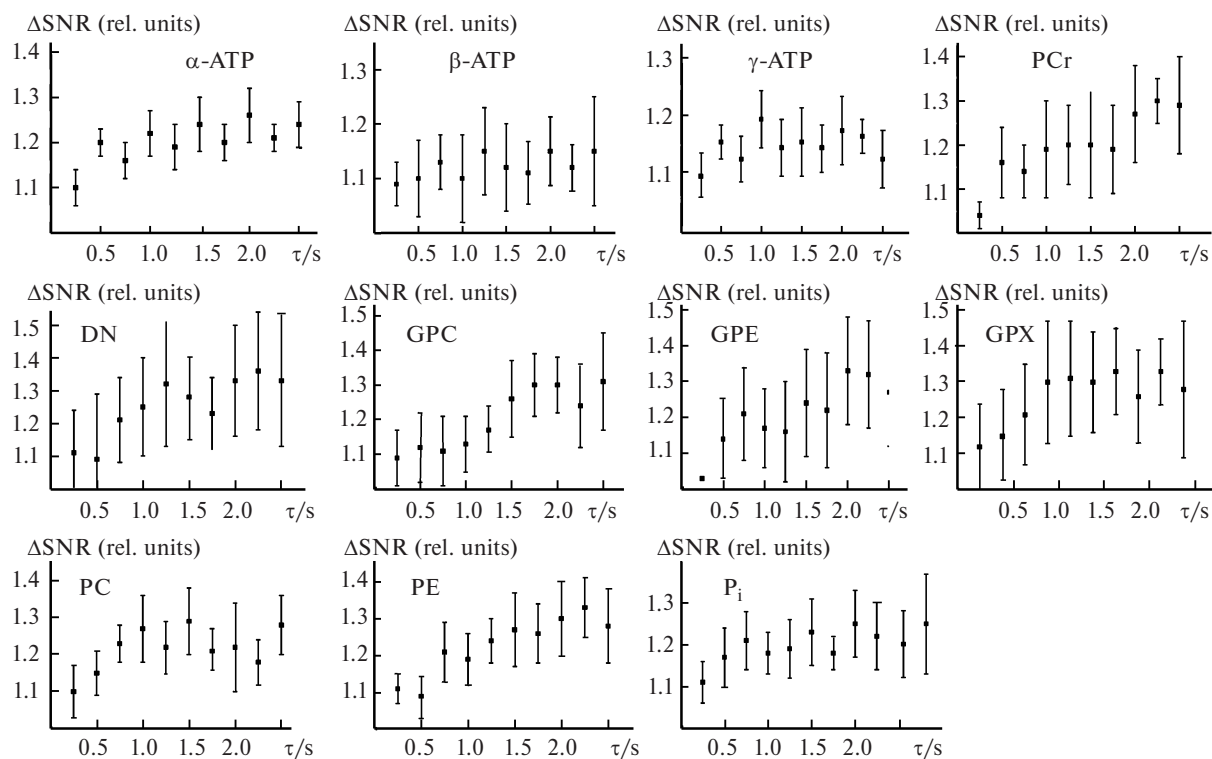
**Results of the third set of measurements.** Figure 4 presents the SNR for different metabolites as a function of the mixing time. Noteworthy is a common trend, namely, an

**Table 3.** Average SNR gain (SD) achieved upon increase in the parameter TR from 2 s to 3 s (I), from 3 s to 4 s (II) and from 2 s to 4 s (III)

Signal	SNR (%) (SD))		
	I (threshold 18.1%)	II (threshold 13.4%)	III (threshold 41.4%)
PCr	33.0 (4.7)*	11.2 (3.7)	44.8 (9.4)*
$\gamma$ -ATP	18.5 (5.7)*	7.1 (5.8)	27.5 (13.1)
$\alpha$ -ATP	16.4 (7.4)	6.7 (2.1)	29.6 (15.7)
$\beta$ -ATP	15.9 (6.0)	7.2 (4.1)	32.1 (17.1)
$\text{P}_i$	35.3 (11.2)*	18.5 (6.6)*	44.1 (15.5)*
PE	30.1 (13.6)*	11.8 (10.2)	56.6 (19.2)*
PC	23.4 (7.1)*	4.1 (3.1)	42.1 (27.4)*
GPE	37.7 (17.9)*	20.2 (9.5)*	73.6 (28.4)*
GPC	29.3 (16.1)*	11.0 (8.8)	66.5 (31.0)*
GPX	15.0 (11.5)	11.3 (5.1)	37.9 (19.8)
DN	20.1 (5.8)*	9.4 (4.5)	22.3 (10.5)

\* Statistically significant gain ( $p < 0.05$  according to Mann–Whitney U-test) that exceeds the effectiveness threshold (for details, see text).

increase in SNR with increasing mixing time. The SNR values for the resonance lines of ATP, PC, GPC, GPX, and DN increase more slowly as the mixing times fall in the range of 1.25–1.75 s. The SNR values for PCr,  $\text{P}_i$ , GPE, and PE increase up to the mixing times of 2.25–2.5 s.

**Fig. 4.** Relative changes in SNR for all metabolites detected in  $^{31}\text{P}$  magnetic resonance spectrum plotted vs. mixing time ( $\tau$ ).

The maximum SNR gain induced by the NOE was 20–35% depending on the metabolite.

**Analysis of the results obtained in the first set of measurements.** From the data shown in Tables 1 and 2 it follows that proton decoupling and NOE applied separately reliably improve the SNR only for certain signals in the  $^{31}\text{P}$  spectrum. Statistically significant SNR gain for all resonance lines in the  $^{31}\text{P}$  spectrum, except the signals of  $\beta$ -ATP and GPX, is achieved by combined use of proton decoupling and NOE. Although these two processes are implemented using the same hardware unit of a MRI scanner, namely, a RF coil operating at the proton resonance frequency, they are separated in time, *viz.*, irradiation to implement the NOE precedes the application of the  $^{31}\text{P}$  excitation pulse while proton decoupling follows the detection of the FID; therefore, both of them can/could and should be used in the same experiment. In this case, protons will be irradiated almost continuously, with only break after application of the Waltz 4 PS used for proton decoupling (see Fig. 2).

**Analysis of the results obtained in the second set of measurements.** Often, it is impossible to vary the parameter NSA in MRS by a few units. This is related to the fundamental properties of pulse sequences. Applying certain excitation RF pulses in the prescribed order is insufficient because of phase changes in the spin system after application of each new RF pulse; as a result, dephasing occurs and the spectrum becomes inappropriate for processing.<sup>13</sup> The spin phase can be maintained constant using phase cycling, *i.e.*, by systematically changing the phase of the excitation pulses and the signal receiver.<sup>13</sup> The single-voxel ISIS PS (see Fig. 2) includes three inversion pulses and thus requires  $2^3 = 8$  phase cycles, *i.e.*, at least eight NSA. The 2D ISIS PS includes one inversion pulse and thus two phase cycles are necessary. Four phase cycles are needed for optimum implementation of the Waltz 4 PS for proton decoupling.<sup>14</sup> Thus, single-voxel spectroscopy requires at least  $8 \cdot 4 = 32$  NSA while 2D spectroscopy needs  $2 \cdot 4 = 8$  NSA.

As a result, the minimum NSA increment appears to be large, which significantly increases the duration of the examination procedure. Therefore, it is impossible to considerably reduce the study time by a slight decrease in the TR because this decrease should be large. In this connection, a question arises as to how large will be the loss of the signal due to incomplete  $T_1$  relaxation of  $^{31}\text{P}$  nuclei upon reducing the time TR.

To evaluate the loss, we carried out the second set of measurements. It is known that  $\text{SNR} \sim \sqrt{\text{NSA}}$ .<sup>15</sup> However, the larger the TR value the smaller the NSA value is needed to maintain the acquisition time. Our task is to determine whether the SNR gain due to the increased time TR will be high enough to compensate the loss originating from the decrease in NSA. On going from TR = 2 s to TR = 3 s the parameter NSA should be decreased by 33.3% and the

SNR will automatically decrease  $\sim 18.1\%$ . This value acts as the effectiveness threshold. Namely, if, at the same NSA value, the SNR gain due to the increase in the time TR from 2 s to 3 s will exceed a value of 18.1%, the longer time TR is preferred. The effectiveness thresholds for the other two cases are obtained analogously. They are equal to 13.4% for the increase in the time TR from 3 s to 4 s and 41.4% for the increase in TR from 2 s to 4 s.

In accordance with the reasoning described above the results of the first set of measurements (see Table 3) show that the value TR = 3 s is more appropriate than TR = 2 s because the SNR gain exceeds the threshold value for most metabolites. The reason is that the time ( $5T_1$ ) necessary for complete relaxation of the metabolites detected in the  $^{31}\text{P}$  magnetic resonance spectrum of the human brain (except ATP) is longer than TR = 2 s. The times  $T_1^*$  of these metabolites are listed below.

$^{31}\text{P}$ MRS metabolite	$T_1/s$ (see Ref. 11)
PE	$6.33 \pm 1.10$
PC	$4.31 \pm 1.04$
$\text{P}_i$	$3.70 \pm 0.46$
GPE	$6.79 \pm 0.95$
GPC	$5.82 \pm 0.88$
PCr	$3.39 \pm 0.17$
DN	$2.07 \pm 0.13$
$\gamma$ -ATP	$1.70 \pm 0.15$
$\alpha$ -ATP	$1.35 \pm 0.14$
$\beta$ -ATP	$1.13 \pm 0.09$

The shorter  $T_1$  the smaller the SNR gain with increasing TR. Indeed, a small SNR gain for ATP found in this work agrees with the fact that the times  $T_1$  for the three resonance lines of ATP are shorter than those of other metabolites.

A comparison of the results obtained using TR = 4 s and 3 s shows that for most metabolites the SNR gain is insufficient to compensate the loss due to the decrease in NSA. This statement is not valid for the peaks of  $\text{P}_i$  and GPE, being consistent with the fact that the times  $T_1$  for the signals of  $\text{P}_i$  and GPE are among the longest relaxation times. Noteworthy is that the SNR gain for PE and PC proved to be smaller than the effectiveness threshold equal to 13.4%, although it was close to this value. This can be explained by difficulties in processing of the (individual) signals of PE and PC and by a large scatter of the corresponding  $T_1$  values (see above).

The SNR gain for  $\text{P}_i$  is of great importance from the standpoint of determination of the intracellular pH because the range of changes in this parameter in living systems is narrow.<sup>16</sup> Changes in pH in the brain due to non-damaging effects, *e.g.*, neural activation, are about 1%;<sup>17</sup> therefore, they can leave undetected due to the low  $\text{SNR}_{\text{P}_i}$  value.

\*The parameter  $T_1$  is the time corresponding to transition of a total of 63% of initially excited nuclei to the equilibrium ground state through  $T_1$ -relaxation.

A comparison of the results obtained for TR = 4 s and 2 s demonstrates the efficiency of the longer TR for the peaks of lipids, PCr, and  $\text{P}_i$ , but not for the peaks of ATP and DN. It follows that TR = 4 s should be used to provide a maximum SNR for the peak of  $\text{P}_i$  and in the studies of lipid exchange. The efficiency of the longer TR for PCr is of less importance because this signal in the spectrum of the human brain has the highest SNR and quantitative processing of the corresponding resonance line presents no difficulties.

Eventually, the best repetition time is TR = 3 s. This contradicts the data reported in Ref. 18 whose authors state that the SNR at TR < 4 s remains too low without increasing the acquisition time. Unfortunately, no quantitative analysis of the results obtained in that study was reported. We have shown that an increase in TR from 3 to 4 s at the same acquisition time causes no high SNR gain for most metabolites. Moreover, energy metabolism alone can be analyzed using TR  $\leq$  2 s and not too large NSA values, thus reducing the study time. For instance, in a study of response of the visual cortex of the human brain in patients with schizophrenia to video stimulation,<sup>3</sup> which required spectra acquisition within the shortest possible time (it was shortened to 6 min), we revealed deviations in energy metabolism using TR = 1.2 s. Unfortunately, low intensity of the signal of  $\text{P}_i$  precluded reliable determination of changes in the intracellular pH ( $\text{pH}_{\text{int}}$ ), which were expected to occur (see, e.g., Ref. 17).

**Analysis of the results obtained in the third set of measurements.** The longer the time TR the longer the time of irradiation at the proton frequency before application of the excitation pulse at the  $^{31}\text{P}$  frequency. During the irradiation dipole-dipole coupling between  $^{31}\text{P}$  nuclei and protons causes the population difference between the excited and non-excited magnetic energy levels of  $^{31}\text{P}$  nuclei to increase. Therefore, a larger number of  $^{31}\text{P}$  nuclei contribute to the resonance signal after irradiation at the phosphorus resonance frequency compared to the experiment without the preliminary step. This is the case for heteronuclear NOE.

The maximum theoretically achievable value of heteronuclear NOE equals half the ratio of the gyromagnetic ratios of proton and phosphorus nucleus,<sup>7</sup> i.e., about 124%. However, since direct dipole-dipole coupling depends strongly on the internuclear distance ( $r$ ), being proportional to  $r^{-6}$ , such a high enhancement cannot be actually attained. The NOE can be practically implemented using two fundamentally different methods.<sup>7</sup> The first, non-stationary NOE, involves a single inversion of proton spins followed by a mixing time before application of the  $^{31}\text{P}$  excitation pulse. In the second method, stationary NOE, the proton system is continuously irradiated during the mixing time with pulses whose power is proportional to the coupling constant. In both cases, the energy of the

proton system is transferred to phosphorus nuclei by the cross-relaxation mechanism during the mixing time. However, in the case of non-stationary NOE this process begins to compete with spin-lattice ( $T_1$ ) relaxation as the mixing time increases. This is not a problem for stationary NOE since the population of the excited level of protons is maintained constant and the dipole-dipole coupling also occurs continuously. Therefore, theoretically one can expect that the population difference between the phosphorus energy levels, which governs the SNR, will monotonically increase until the equilibrium state is attained.

The plots of the results obtained in the third set of measurements (see Fig. 4) show that for most metabolites a noticeable SNR gain due to the NOE could not be observed at mixing times longer than 1.5 s. The exceptions are PCr,  $\text{P}_i$ , PE, and GPE for which the SNR gain increases to a mixing time of nearly 2.5 s. Since the NOE depends crucially on the internuclear distance, the difference between the maximum achievable SNR gain corresponding to the stationary state is determined by the structure of the phosphorus-containing molecule and by its solvability. The shorter the distance between the  $^{31}\text{P}$  nucleus and a water proton striving to be involved in the dipole-dipole coupling with this nucleus the more pronounced the NOE.

The maximum mixing time is determined by the parameter TR. Assuming that TR = 3 s, signal acquisition after excitation at the  $^{31}\text{P}$  resonance frequency takes about 0.5 s, so the mixing time is limited to nearly 2.5 s. This is sufficient to obtain the maximum SNR gain induced by the NOE for almost all metabolites.

Summing up, we have shown that proton decoupling and NOE should be used in combination. The time TR = 3 s is optimum for  $^{31}\text{P}$  MRS of the human brain.

Indeed, owing to low  $T_1$ -weighting of the spectra, one can reach the optimum SNR for most metabolites on the one hand and achieve a considerable SNR gain of 20–35% for different metabolites due to the long NOE mixing time on the other hand. Other values of the parameter TR may also appear to be appropriate depending on the particular task. An increase in TR to 4 s and subsequent decrease in  $T_1$ -weighting of the spectrum, as well as the mixing time increased to 3.5 s will contribute to the SNR gain for PCr,  $\text{P}_i$ , PE, and GPE; however, no positive effect will be attained for other peaks. Therefore, it is advisable to use the value TR = 4 s for the most accurate determination of intracellular pH and for analysis of deviations in the phospholipid profiles. Of two TR values, 2 s and 4 s, the former is preferable if researchers are aimed at analyzing energy metabolism alone. Indeed, this will lead to an increase in the SNR for the signals accessible to analysis of macroergic phosphates without loss of the SNR gain induced by the NOE and will not increase the study duration.

## References

1. A. Sato, M. Kataoka, Y. Kuwabara, M. Kimura, Y. Seo, A. Masaoka, *J. Surg. Res.*, 1996, **61**, 373.
2. T. E. Merchanta, J. N. Kasimos, T. Vroom, E. de Bree, J. L. Iwata, P. W. de Graaf, T. Glonek, *Cancer Lett.*, 2002, **176**, 159.
3. A. V. Manzhurtsev, N. A. Semenova, M. V. Ublinskii, T. A. Akhadov, S. D. Varfolomeev, *Russ. Chem. Bull.*, 2016, **65**, 1630.
4. F. Du, A. J. Cooper, T. Thida, S. Sehovic, S. E. Lukas, B. M. Cohen, X. Zhang, D. Ongür, *JAMA Psychiatry*, 2014, **71**, 19.
5. O. A. Petroff, J. W. Prichard, K. L. Behar, J. R. Alger, J. A. den Hollander, R. G. Shulman, *Neurology*, 1985, **35**, 781.
6. P. B. Barker, X. Golay, D. Artemov, R. Ouwkerk, M. A. Smith, A. J. Shaka, *Magn. Res. Med.*, 2001, **45**, 226.
7. T. D. W. Claridge, *High-Resolution NMR Techniques in Organic Chemistry*, 3rd ed., Ch. 9, *Correlations Through Space: The Nuclear Overhauser Effect*, Elsevier, Oxford, UK, 2016, 552 pp.
8. A. L. L. Kolkovsky, in *<sup>1</sup>H and <sup>31</sup>P NMR Spectroscopy for the Study of Brain Metabolism at Ultra High Magnetic Field from Rodents to Men*, Université Paris Sud, Paris XI, 2015, Ch. 1.2.4, p. 39.
9. P. Prasad, *Magnetic Resonance Imaging: Methods and Biologic Applications*, Springer Science and Business Media, New York, 2006, Ch. 2.4.1.3, p. 230.
10. *Magnetic Resonance Spectroscopy*, Eds. Ch. Stagg, D. Rothman, Elsevier, Oxford, 2013, Ch. 1.2, p. 25–26.
11. J. Ren, A. D. Sherry, C. R. Malloy, *NMR Biomed.*, 2015, **28**, 1455.
12. A. J. Shaka, J. Keeler, T. Frenkiel, R. Freeman, *J. Magn. Reson.*, 1983, **52**, 335.
13. J. Keller, *Understanding NMR Spectroscopy*, 2nd ed., University of Cambridge, Wiley, Cambridge, 2010, Ch. 9, p. 9-1.
14. R. Freeman, E. Kupce, *NMR Biomed.*, 1997, **10**, 372.
15. M. H. Levitt, *Spin Dynamics: Basics of Nuclear Magnetic Resonance*, 2nd ed., The University of Southampton, UK, Wiley, Southampton, 2008, Ch. 5.2, p. 86–89.
16. M. Chesler, *Physiol. Rev.*, 2003, **83**, 1183.
17. V. A. Magnotta, H.-Y. Heo, B. J. Dlouhy, N. S. Dahdaleh, R. L. Follmer, D. R. Thedens, M. J. Welsh, J. A. Wemmie, *PNAS*, 2012, **109**, 8270–8273.
18. J. Novak, M. Wilson, L. MacPherson, T. N. Arvanitis, N. P. Davies, A. C. Peet, *Eur. J. Radiology*, 2014, **83**, e106–e112.

Received June 13, 2017;  
in revised form October 16, 2017;  
accepted December 14, 2017